Shock synthesis of quasicrystals with implications for their origin in asteroid collisions

Paul D. Asimow[a,1], Chaney Lin[b], Luca Bindi[c,d], Chi Ma[a], Oliver Tschauner[e,f], Lincoln S. Hollister[g], and Paul J. Steinhardt[b,h]

[a]Division of Geological and Planetary Sciences, California Institute of Technology, Pasadena, CA 91125; [b]Department of Physics, Princeton University, Princeton, NJ 08544; [c]Dipartimento di Scienze della Terra, Università degli Studi di Firenze, I-50121 Firenze, Italy; [d]Consiglio Nazionale delle Ricerche–Istituto di Geoscienze e Georisorse, Sezione di Firenze, I-50121 Firenze, Italy; [e]Department of Geoscience, University of Nevada, Las Vegas, NV 89154; [f]High Pressure Science and Engineering Center, University of Nevada, Las Vegas, NV 89154; [g]Department of Geosciences, Princeton University, Princeton, NJ 08544; and [h]Princeton Center for Theoretical Science, Princeton University, Princeton, NJ 08544

Edited by Mark H. Thiemens, University of California, San Diego, La Jolla, CA, and approved May 6, 2016 (received for review January 7, 2016)

We designed a plate impact shock recovery experiment to simulate the starting materials and shock conditions associated with the only known natural quasicrystals, in the Khatyrka meteorite. At the boundaries among $CuAl_5$, $(Mg_{0.75}Fe^{2+}_{0.25})_2SiO_4$ olivine, and the stainless steel chamber walls, the recovered specimen contains numerous micron-scale grains of a quasicrystalline phase displaying face-centered icosahedral symmetry and low phason strain. The compositional range of the icosahedral phase is $Al_{68–73}Fe_{11–16}Cu_{10–12}Cr_{1–4}Ni_{1–2}$ and extends toward higher Al/(Cu+Fe) and Fe/Cu ratios than those reported for natural icosahedrite or for any previously known synthetic quasicrystal in the Al-Cu-Fe system. The shock-induced synthesis demonstrated in this experiment reinforces the evidence that natural quasicrystals formed during a shock event but leaves open the question of whether this synthesis pathway is attributable to the expanded thermodynamic stability range of the quasicrystalline phase at high pressure, to a favorable kinetic pathway that exists under shock conditions, or to both thermodynamic and kinetic factors.

icosahedrite | shock metamorphism | alloys | meteorites | quasicrystals

Quasicrystals are solids with rotational symmetries forbidden for crystals (1, 2). Quasicrystals can be synthesized in the laboratory by mixing precise ratios of selected elemental components in the liquid and quenching under strictly controlled conditions ranging from rapid to moderately slow (3, 4). Nonetheless, the finding of two natural quasicrystals (5–8) in the Khatyrka meteorite (9), which displays clear evidence of a shock generated by a high-velocity impact event (10), introduced a dramatic new possible mechanism of quasicrystal formation. Here, we report the results of a shock recovery experiment designed to reproduce some aspects of a collision that may have occurred between extraterrestrial bodies.

Icosahedrite is only stable on the liquidus of the Al-Cu-Fe system in a narrow compositional range and only between 700 °C and 850 °C at ambient pressure (11), but its stability field is enlarged in static high-pressure conditions, where it has been observed in experiments quenched from 1,400 °C at 21 GPa (12). The presence of other high-pressure phases (ahrensite and stishovite) (10) associated with shocks, adjacent to icosahedrite and decagonite in the Khatyrka CV3 carbonaceous chondrite, together with the static high-pressure stability of the quasicrystalline phase, are suggestive of an origin during the high-pressure pulse of a shock event. However, there are numerous differences between the static high-pressure, high-temperature conditions studied by Stagno et al. (12) and shock-induced conditions at nominally similar peak (P, T) conditions—including heterogeneous and rapidly time-varying pressure and temperature fields (13, 14), typical adiabatic decompression rather than temperature quench at high pressure (15), and hypersonic turbulent shear flows (16–18). A direct demonstration of synthesis of an Al-Cu-Fe icosahedral quasicrystal from discrete starting materials in a laboratory shock recovery experiment would offer substantial new evidence in favor of the shock-induced origin of the natural example and potentially may provide uniquely precise constraints on the shock conditions experienced in the Khatyrka meteorite.

Observations of the Khatyrka meteorite specimens show that Cu-Al–rich alloys are present as well as phases typical of CV3 carbonaceous chondrites, including Fe-bearing olivine and FeNi metal (9). The source of Fe in the icosahedrite is unclear. Hence we designed an experiment to test simultaneously whether Al-Cu-Fe alloys, quasicrystalline or not, can form by shock processing of Cu-Al in contact with Fe^{2+}-bearing silicates or from Cu-Al in contact with Fe-rich metals. A stack of target discs, each 5 mm in diameter and 0.5–1.0 mm thick, were loaded into a cavity 5 mm below the impact surface of a stainless steel 304 (SS304) ($Fe_{71}Cr_{18}Ni_8Mn_2Si_1$) vented recovery chamber. In order along the shock propagation direction, the discs were $(Mg_{0.75}Fe_{0.25})_2SiO_4$ olivine, $CuAl_5$ alloy, natural FeNi from the Canyon Diablo meteorite, and $Al_{14}Cu_4Fe_1Ni_1$ alloy. The target was impacted by a 2-mm-thick Ta flyer launched at 896 ± 4 m s^{-1}, generating a shock event with a duration of 500 ns and peak shock pressures in the various layers ranging from 14 to 21 GPa. The chamber was recovered intact, sawn open along a plane parallel to the shock direction, polished, and examined by scanning electron microscopy (SEM), electron backscatter diffraction (EBSD), and electron probe microanalyzer. One grain displaying pentagonal symmetry in EBSD was plucked from the exposed surface, mounted on a carbon fiber, and analyzed by single-crystal and powder X-ray diffraction (XRD).

Results

A general reflected-light view of one-half of the polished surface of the recovered specimen is shown in Fig. 1. Little if any transformation

Significance

The singular occurrence, to date, of natural quasicrystals requires an explanation both of the possibility and of the rarity of their formation outside of the laboratory. Successful synthesis by an experimental shock, with starting materials similar to the exotic intermetallic alloys in the Khatyrka meteorite, demonstrates a mechanism that is feasible in space but not in any natural setting on Earth. The previously unrecognized composition of the synthesized quasicrystal, the first, to our knowledge, to be created by shocking discrete bulk starting materials, demonstrates a method for discovery of previously unknown quasicrystal compositions.

Author contributions: P.D.A. and P.J.S. designed research; P.D.A., C.L., L.B., C.M., and O.T. performed research; P.D.A., C.L., L.B., C.M., O.T., and L.S.H. analyzed data; and P.D.A., L.B., and P.J.S. wrote the paper.

The authors declare no conflict of interest.

This article is a PNAS Direct Submission.

Data deposition: Crystallographic data on quasicrystals is available from the authors upon request.

[1]To whom correspondence should be addressed. Email: asimow@gps.caltech.edu.

This article contains supporting information online at www.pnas.org/lookup/suppl/doi:10.1073/pnas.1600321113/-/DCSupplemental.

or reaction is observed in the interiors of the target layers or along most of the interfaces in the region of one-dimensional flow near the center of the capsule (toward the right side of the image). Along the outer circumference of the chamber, however, a channel about 1 mm wide displays a strong shear flow or jet with transport of material more than 1 mm down-range from its starting point. The texture shows angular fragments of olivine grading into rounded spherules surrounded by metal of a color and backscattered electron contrast (Fig. 2) distinct from any of the starting materials or chamber wall. We focus here on a region at the boundary between the unmodified $CuAl_5$ layer and the newly formed hybrid metal region, close to the edge of the olivine layer and containing numerous rounded nonmetallic inclusions. At the leading edge of interaction between the Fe-rich metal and the $CuAl_5$ metal, in intimate contact with rounded blobs of olivine and spinel-like composition, we found a region labeled i-phase in Fig. 2*C* that displays a pentagonal symmetry in its Kikuchi pattern obtained by EBSD (Fig. 3, *Upper*). The EBSD software, which is designed to index crystalline phases, was unable to index this pattern in any standard crystal system. Electron microprobe analysis of this grain yields the composition shown in Table 1: on an atomic basis, $Al_{72}Fe_{16}Cu_{10}Cr_1Ni_1$. Two other grains found on the opposite side of the capsule (in similar position relative to the $CuAl_5$, rounded olivine and spinel-composition regions, and SS304 starting materials) yield similar compositions with measurable concentrations of all five of these elements and display the pentagonal symmetry in their EBSD Kikuchi pattern. Noting that none of the starting materials contains all of the elements found in the i-phase, a reaction during the experiment involving at least two of the starting materials was necessary to form this phase. The simplest explanation, given the presence of Cr and Ni, is that the i-phase formed by reaction of the $CuAl_5$ and SS304, but only in the presence of or on the surfaces of olivine or spinel-like melt globules derived from the olivine by reduction of Fe and Si coupled to oxidation of Al (Fig. S1). The FeNi and $Al_{14}Cu_4Fe_1Ni_1$ layers did not appear to have contributed material to the region of quasicrystal formation; they may not have reached high enough temperature to melt, mix, or react.

After analysis in polished section, a single grain from the area shown in Fig. 2*C* was extracted, attached to a carbon fiber, and

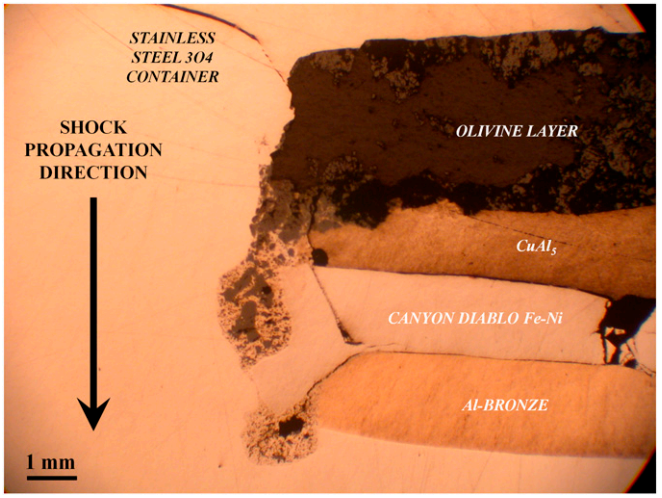

Fig. 1. Reflected light photomicrograph of shock recovery experiment S1230. Labels indicate direction of shock propagation and layout of discs of starting material in deformed cavity within container. The area of interest where layers mixed and reacted is near the center of the image. Dark areas are where material was plucked from the surface during polishing; there were no voids or vesicles in the sample as recovered.

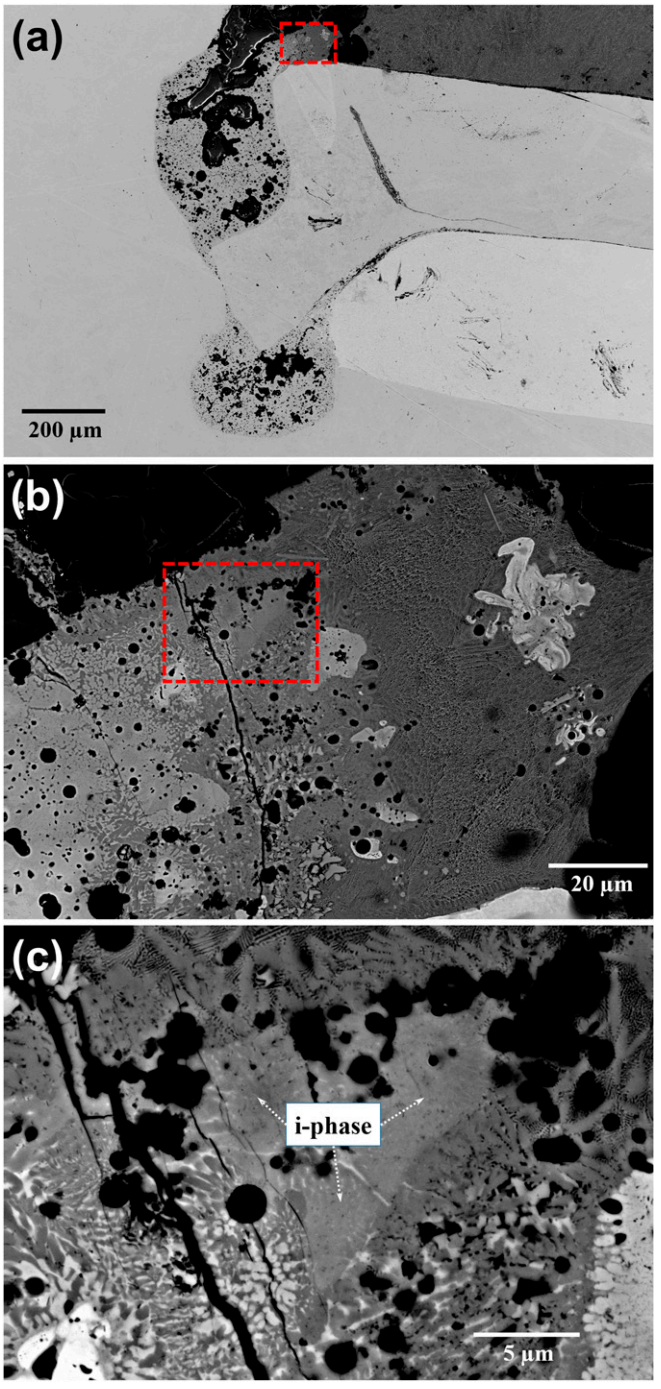

Fig. 2. Backscattered electron images of recovered sample; contrast is stretched to emphasize differences among metals, which leaves areas of olivine and spinel composition dark. Dark areas are not voids, except in a few places where material was plucked during polishing. (*A*) The same area as shown in Fig. 1; red dashed box indicates the region to be enlarged. (*B*) The area where $CuAl_5$ (on the right), Fe-rich metal (on the left), and olivine (at top) have mixed and reacted; red dashed box indicates the region to be enlarged. (*C*) At high magnification, the icosahedral quasicrystals are indicated by the label "i-phase." The i-phase at upper right corresponds to the first analysis in Table 1, the EBSD pattern in Fig. 3, *Upper* and the subject of XRD study in Fig. 3, *Lower* and Table 2. The dark regions in this image are mostly close to $MgAl_2O_4$ composition; some are close to Mg_2SiO_4. Some dark regions are crystalline, and some appear to be amorphous.

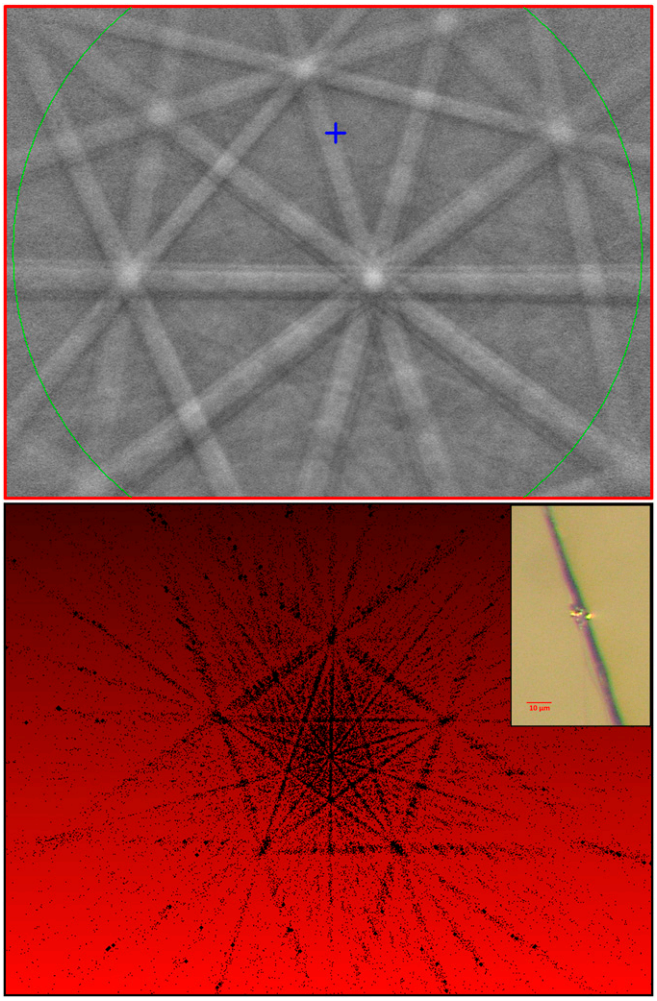

Fig. 3. Diffraction results for the i-phase. (*Upper*) Electron backscatter diffraction pattern of the i-phase region indicated in Fig. 2*C*, showing pentagonal zone axis. (*Lower*) Single-crystal XRD pattern in gnomonic projection down the fivefold rotational axis; the extracted grain attached to a carbon fiber is shown in the *Inset*.

analyzed by both single-crystal and powder XRD. The single-crystal pattern, in gnomonic projection, is shown in Fig. 3, *Lower* (Precession figures down the fivefold, threefold, and twofold axes are given in Fig. S2). It displays precisely the same rotational axes and overall face-centered icosahedral symmetry as natural icosahedrite and low phason strain. This low phason strain is contrary to the typical appearance of metastable quasicrystals grown by rapid quenching from melt, which exhibit phason strain that manifests as diffraction peaks that are broadened and shifted systematically from the ideal icosahedrally symmetric pattern (19, 20). The peaks in the powder diffraction pattern, indexed on the basis of six integer indices conventionally used with quasicrystals (3, 4), are listed in Table 2 and compared with the corresponding peaks in the isostructural natural icosahedrite $Al_{63}Cu_{24}Fe_{13}$ (5, 6). All of the same peaks are identified but are systematically shifted to larger *d*-spacing (the powder patterns are compared in Fig. S3). In detail, the second figure-of-merit test introduced by Lu et al. (21) to compare the observed intensities to those of an ideal quasicrystal can be used as a sensitive quantitative test of phason strain. The intensities measured for the i-phase produced in our shock experiment are nearly identical to those observed for icosahedrite (5), which scored as well as the best laboratory specimens. The pattern is consistent with a six-dimensional cell parameter $a_{6D} = 12.71(3)$ Å, which plots on an extension of the linear correlation between a_{6D} and Al/Cu ratio established in previously observed Al-Cu-Fe quasicrystals in the range of $12.62 < a_{6D} < 12.64$ Å (22). The substantial grain size (up to 10 μm) and low phason strain seem inconsistent with the timescale of the high-pressure pulse, ~500 ns; more likely, even if nucleation occurred at peak pressure, quasicrystal growth and annealing continued after pressure release until the millimeter-scale, high-temperature region associated with strong shear flow and melting was cooled by conduction to adjacent low-temperature areas.

Discussion

The results of our shock synthesis experiment answer some questions and raise others. Most significantly, as the first, to our knowledge, documented shock synthesis of a quasicrystal from discrete bulk starting materials, it lends support to the hypothesis that the quasicrystals found in the Khatyrka meteorite formed as a result of hypervelocity impacts among objects in the early Solar system. We note that this synthesis was successful on the first attempt. However, the experiment does not explain the ultimate origin of Cu-Al alloys in the Khatyrka precursor or whether the source of Fe is direct incorporation from Fe-rich metal or reduction of Fe^{2+} from neighboring minerals.

Notably, our shock synthesis process has produced a new type of quasicrystal with composition and lattice parameter (a_{6D}) distinct from all previously known quasicrystals in the Al-Cu-Fe family. In terms of explaining natural icosahedrite, the compositional difference suggests that some combination of the starting materials, pressure–temperature–time history, or flow field in the experiment was not a perfect match to the conditions of the natural shock. As a novel synthesis procedure, our work suggests that shocking combinations of discrete bulk materials [in contrast to shocking homogenized powders with compositions matching previously known quasicrystals (23)] may prove to be a useful pathway for discovering new quasicrystals and developing a better understanding of their kinetic and thermodynamic stability.

Methods

Shock Recovery Experiment. A stack of starting material discs, each 5 mm in diameter, were loaded in a SS304 (18 wt% Cr, 8 wt% Ni, <2 wt% Mn, < 1 wt% Si, and < 0.08 wt% C) chamber. The starting materials were, in order in the direction of shock propagation: 1.0-mm-thick synthetic olivine $(Mg_{0.75}Fe_{0.25})_2SiO_4$, 0.5-mm-thick $CuAl_5$ alloy (initial microstructure is a mix of $CuAl_2$ theta

Table 1. Electron microprobe analyses for three regions of the icosahedral phase

	Area 1	Area 2	Area 3
n	4	3	4
Wt%			
Al	54.7 (13)	56.2 (6)	49.3 (2)
Fe	24.6 (7)	17.9 (4)	23.1 (2)
Cu	17.3 (5)	20.9 (2)	19.30 (9)
Cr	1.48 (3)	4.03 (6)	5.22 (6)
Ni	2.02 (6)	1.85 (8)	2.55 (8)
Total	100.0 (18)	100.9 (7)	99.5 (1)
Atomic%, normalized			
Al	72.3 (5)	73.3 (4)	67.94 (13)
Fe	15.7 (5)	11.3 (3)	15.42 (13)
Cu	9.7 (1)	11.57 (5)	11.30 (6)
Cr	1.02 (3)	2.73 (6)	3.73 (5)
Ni	1.23 (3)	1.11 (5)	1.62 (5)
Total	100	100	100

n is the number of spot analyses in each average. Uncertainty in the least significant digits is shown in parentheses [e.g., 72.3 (5) = 72.3 ± 0.5].

Table 2. X-ray powder-diffraction data for icosahedrite and synthetic i-phase obtained in the shock experiment

I_{rel}	Icosahedrite	Synthetic i-phase	n_i	(*N*, *M*)
2	8.94	8.99	200000	(8, 4)
5	5.53	5.58	$11\bar{1}\bar{1}11$	(12, 16)
20	3.75	3.81	200022	(24, 36)
25	3.41	3.46	$31\bar{1}\bar{1}11$	(28, 44)
20	3.24	3.28	220022	(32, 48)
5	2.799	2.854	$31\bar{1}\bar{1}31$	(44, 64)
10	2.451	2.508	420022	(56, 84)
5	2.350	2.404	$31\bar{1}\bar{1}33$	(60, 92)
90	2.108	2.148	$42\bar{2}\bar{2}22$	(72, 116)
100	2.006	2.052	$40\bar{2}042$	(80, 128)
5	1.728	1.770	$53\bar{1}\bar{1}33$	(108, 172)
15	1.452	1.498	$62\bar{2}044$	(152, 244)
5	1.418	1.462	$62\bar{2}\bar{2}44$	(160, 256)
30	1.238	1.291	$60\bar{4}064$	(208, 236)

d-spacings of indexed peaks are given in Ångstroms. The patterns were indexed on the basis of the integer linear combinations of the six vectors (g_k, g_5); the last column is an equivalent two-integer index introduced by Janot (equations 3.20–3.26 in ref. 3).

phase and FCC Al), 0.5-mm-thick natural FeNi from the Canyon Diablo type I-A iron meteorite (containing lamellae of kamacite and taenite and possibly some schreibersite, although no inclusions were visible on either surface of the disk), and 0.5-mm-thick Al-bronze alloy (homogenous $Cu_{14}Al_4Fe_1Ni_1$). The method of assembly typically leaves voids ∼10 μm in size around the outer radius of the sample cavity, ∼1 μm in size along the front and back faces of the chamber, and ∼0.1 μm in size between polished discs of the sample stack. The target was struck by a 2.0-mm-thick Ta flyer plate attached to the front of a polycarbonate sabot and launched at 896 ± 5 m s^{-1} by a single-stage 20-mm bore propellant gun. The shock propagated through an initially 5-mm-thick SS304 driver and then into the sample cavity. The crater formed on the recovered surface of the driver was <1 mm deep. Simple impedance-matching calculations suggest that the first shock conditions in the [SS304, olivine, $CuAl_5$, FeNi, and Al-bronze] layers were, respectively, particle velocity = [510, 584, 717, 514, 545] ± 4 m s^{-1}, shock velocity = [5.33, 6.97, 6.07, 4.56, and 5.08] ± 0.006 km s^{-1}, and pressure = [21.4, 17.9, 13.7, 18.4, 17.0] ± 0.1 GPa. Conventional shock-temperature estimates do not exceed 400 °C in any of the layers. The duration of the supported shock is such that the reflected shock from the $CuAl_5$-FeNi impedance jump returned to the front surface of the olivine layer at the same time as the leading edge of the release wave from the back of the flyer. Hence, the olivine and $CuAl_5$ layers experienced two shocks, with peak pressures ∼20 GPa in the olivine and 16 GPa in the $CuAl_5$. The total duration between first shock and release was close to 500 ns throughout the sample stack. At the radial boundaries of the sample stack, machining gaps allowed substantial shear flow, with brecciation followed by melting and material transport distances as large as 1 mm. Temperatures in this region were sufficient, based on intermingling textures and spherical droplet formation, to melt both metal and silicate materials either on shock or, more likely, upon release, but it is unclear how to quantify the peak temperature. Most of the interesting reactions occurred in the boundary region in or near these areas of large shear flow (as evident in Figs. 1 and 2). We wish to point out that, in interpreting these images, the dark areas are not to be mistaken for voids or vesicles; they are filled with low-Z oxide or silicate material. Although, in a previous experiment at somewhat higher pressure and longer duration, we found transformation of olivine to the high-pressure polymorph wadsleyite (24), recovery of such polymorphs in experiments is exceedingly rare. Despite an extensive search by means of synchrotron XRD maps and electron backscatter diffraction experiments, we found no high-pressure silicate polymorphs in the present sample.

SEM. The sample was sawn in half with a water-cooled diamond wafering blade along a plane parallel to the shock propagation direction. One side of the recovered charge was impregnated with epoxy and mechanically polished in flowing water with Al_2O_3-abrasive papers down to 5 μm and loose diamond powder down to 0.25 μm, followed by 3 h of vibrational polishing in colloidal silica (30 nm in diameter) solution. No carbon coat was applied. The sample was first analyzed at Princeton University's Imaging and Analysis Center on an FEI Quanta 200 Field-Emission Gun Environmental Scanning Electron Microscope equipped with an Oxford INCA Synergy 450 Energy-Dispersive X-ray spectrometer (EDS). These initial analyses identified regions with compositions resembling that of icosahedrite plus minor amounts of Cr and Ni. The sample was then examined on the California Institute of Technology (Caltech) Geological and Planetary Sciences Division (GPS) Zeiss 1550VP field-emission scanning electron microscope equipped with an angle-sensitive backscattered electron detector, a 150-mm^2 active area Oxford X-Max Si-drift-detector EDS, and an HKL electron backscatter diffraction (EBSD) system. Imaging, mapping, semiquantitative EDS analysis, and EBSD of the previously identified regions were conducted using the SmartSEM, AZtec, and Channel 5 softwares packages. Analyses used a 20-kV accelerating potential and a 120-μm field aperture in high-current mode (∼4-nA probe current), yielding imaging resolution better than 3 nm and an activation volume for EDS analysis ∼1 μm^3.

Electron Probe Microanalyzer. After location of the i-phase and identification of major and minor elements by SEM, three regions were reanalyzed for Al, Cu, Fe, Cr, and Ni using wavelength dispersive X-ray spectroscopy on a five-spectrometer JEOL 8200 electron microprobe in the GPS analytical facility at Caltech. High spatial resolution was achieved using conditions of 15 kV, 5 nA, and a focused beam. Pure metal standards were used. Counting times were 20 s on-peak and 10 s each on high and low background positions. Data reduction used the CITZAF routine built into the Probe for Electron Probe Microanalyzer (EPMA) software.

XRD. Studies were performed at the Centro di Studi per la Cristallografia Strutturale, Department of Chemistry, Università di Firenze, Italy. A small fragment (size about 10 × 5 × 5 μm) was extracted from the polished section under a reflected light microscope and mounted on a 5-μm-diameter carbon fiber, which was, in turn, attached to a glass rod. The single-crystal X-ray study was done with an Oxford Diffraction Xcalibur3 CCD single-crystal diffractometer using MoKα radiation (λ = 0.71073 Å) with working conditions of 60 kV and 50 nA and with 450-s exposure time per frame; the detector-to-sample distance was 6 cm. A full Ewald sphere was collected up to $2\theta = 72°$ at room temperature. Data were not corrected for Lorentz or polarization effects or for absorption. Then, to get a powder diffraction pattern, the same grain was studied with an Oxford Diffraction Xcalibur PX Ultra diffractometer equipped with a 165-mm diagonal Onyx CCD detector at 2.5:1 demagnification operating with CuKα radiation (λ = 1.5406 Å). The working conditions were 50 kV and 50 nA with 7 h of exposure; the detector-to-sample distance was 7 cm. Data were processed using the CrysAlis software package version 1.171.36.28 running on the Xcalibur PX control PC.

ACKNOWLEDGMENTS. P.D.A. is supported by US National Science Foundation (NSF) Award EAR-1426526. L.B. is funded with the "60%2013" research funds from the University of Firenze, Italy. C.L. and P.J.S. are supported, in part, by NSF-MRSEC Program Grants DMR-0820341 through New York University and DMR-0819860 through the Princeton Center for Complex Materials. SEM, EDS, EBSD, and EPMA analyses were carried out at the Caltech GPS Division Analytical Facility, which is supported, in part, by NSF Grants EAR-0318518 and DMR-0080065.

1. Shechtman D, Blech I, Gratias D, Cahn JW (1984) Metallic phase with long-range orientational order and no translational symmetry. *Phys Rev Lett* 53(20): 1951–1953.
2. Levine D, Steinhardt PJ (1984) Quasicrystals: A new class of ordered structures. *Phys Rev Lett* 53(26):2477–2480.
3. Janot C (1992) *Quasicrystals: A Primer* (Oxford Univ. Press, Oxford).
4. Bancel PA (1991) Order and disorder in icosahedral alloys. *Quasicrystals: The State of the Art*, eds DiVincenzo DP, Steinhardt PJ (World Scientific, Singapore), pp 17–56.
5. Bindi L, Steinhardt PJ, Yao N, Lu PJ (2009) Natural quasicrystals. *Science* 324(5932): 1306–1309.
6. Bindi L, Steinhardt PJ, Yao N, Lu PJ (2011) Icosahedrite, $Al_{63}Cu_{24}Fe_{13}$, the first natural quasicrystal. *Am Min* 96(5-6):928–931.
7. Bindi L, et al. (2015) Natural quasicrystal with decagonal symmetry. *Sci Rep* 5:9111.
8. Bindi L, et al. (2015) Decagonite, $Al_{71}Ni_{24}Fe_5$, a quasicrystal with decagonal symmetry from the Khatyrka CV3 carbonaceous chondrite. *Am. Min.* 100(10):2340–2343.
9. MacPherson GJ, et al. (2013) Khatyrka, a new CV3 find from the Koryak Mountains, Eastern Russia. *Meteorit Planet Sci* 48(8):1499–1514.
10. Hollister LS, et al. (2014) Impact-induced shock and the formation of natural quasicrystals in the early solar system. *Nat Commun* 5:4040.
11. Zhang L, Lück R (2003) Phase diagram of the Al–Cu–Fe quasicrystal-forming alloy system: I. Liquidus surface and phase equilibria with liquid. *Z Metallk* 94(2):91–97.
12. Stagno V, et al. (2015) Quasicrystals at extreme conditions: The role of pressure in stabilizing icosahedral $Al_{63}Cu_{24}Fe_{13}$ at high temperature. *Am. Min.* 100(11-12):2412–2418.
13. Malavergne V, Guyot F, Benzerara K, Martinez I (2001) Description of new shock-induced phases in the Shergotty, Zagami, Nakhla and Chassigny meteorites. *Meteorit Planet Sci* 36(10):1297–1305.

14. Sharp TG, DeCarli PS (2006) Shock effects in meteorites. *Meteorites and the Early Solar System II*, eds Lauretta DS, McSween HY (Univ. of Arizona Press, Tucson, ZA), pp 653–677.
15. Tomeoka K, Yamahana Y, Sekine T (1999) Experimental shock metamorphism of the Murchison CM carbonaceous chondrite. *Geochim Cosmochim Acta* 63(21):3683–3703.
16. Potter DK, Ahrens TJ (1994) Shock induced formation of $MgAl_2O_4$ spinel from oxides. *Geophys Res Lett* 21(8):721–724.
17. Kenkmann T, Hornemann U, Stöffler D (2000) Experimental generation of shock-induced pseudotachylites along lithological interfaces. *Meteorit Planet Sci* 35(6):1275–1290.
18. Stöffler D, Bischoff A, Buchwald V, Rubin A (1988) Shock effects in meteorites. *Meteorites and the Early Solar System*, eds Kerridge JF, Matthews MS (Univ. of Arizona Press, Tucson, AZ), pp 165–202.
19. Levine D, et al. (1985) Elasticity and dislocations in pentagonal and icosahedral quasicrystals. *Phys Rev Lett* 54(14):1520–1523.
20. Lubensky TC, Socolar JE, Steinhardt PJ, Bancel PA, Heiney P (1986) Distortion and peak broadening in quasicrystal diffraction patterns. *Phys Rev Lett* 57(12): 1440–1443.
21. Lu PJ, Deffeyes K, Steinhardt PJ, Yao N (2001) Identifying and indexing icosahedral quasicrystals from powder diffraction patterns. *Phys Rev Lett* 87(27 Pt 1): 275507.
22. Quiquandon M, et al. (1996) Quasicrystal and approximant structures in the Al-Cu-Fe system. *J Phys Condens Matter* 8(15):2487–2512.
23. Takasaki A, Matsumoto H (2009) Synthesis of Ti-based bulk quasicrystal by shock compression. *Adv Powder Technol* 20(4):395–397.
24. Tschauner O, et al. (2009) Ultrafast growth of wadsleyite in shock-produced melts and its implications for early solar system impact processes. *Proc Natl Acad Sci USA* 106(33):13691–13695.

Supporting Information

Asimow et al. 10.1073/pnas.1600321113

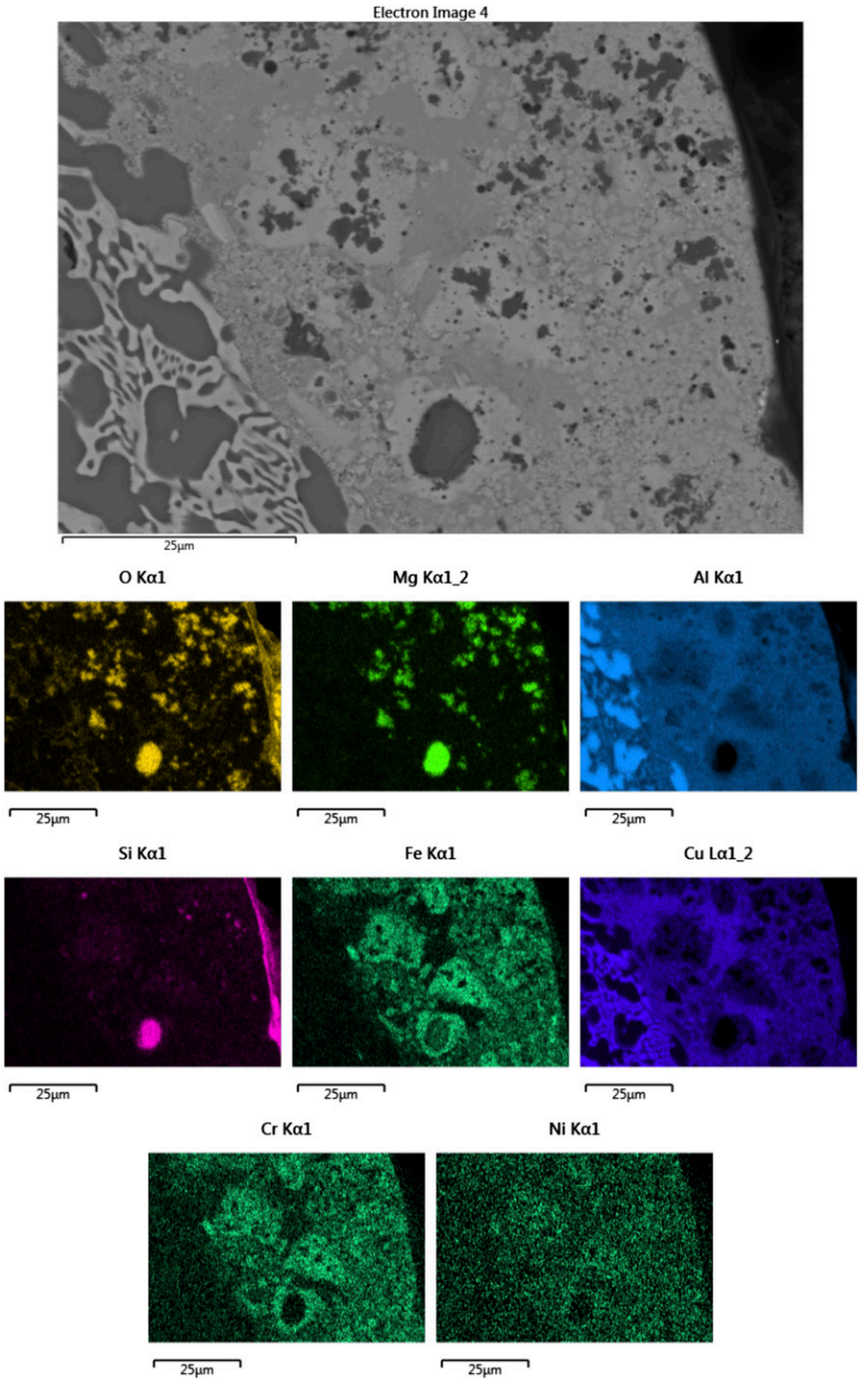

Fig. S1. Backscattered electron image and EDS X-ray intensity maps of an area of mixed metal and silicate; the i-phase forms bright haloes near the image center. The backscatter contrast is set low to show that the dark regions are filled with silicate or oxide material and are not voids. The X-ray maps show that most dark areas are spinel-like, dominated by Mg, Al, and O. However, one large dark area is olivine-like, dominated by Mg, Si, and O. Some of the aluminous regions yield crystalline spinel EBSD or XRD patterns; others appear to be amorphous. The $CuAl_5$ starting material was to the left and the SS304 capsule wall was toward the right.

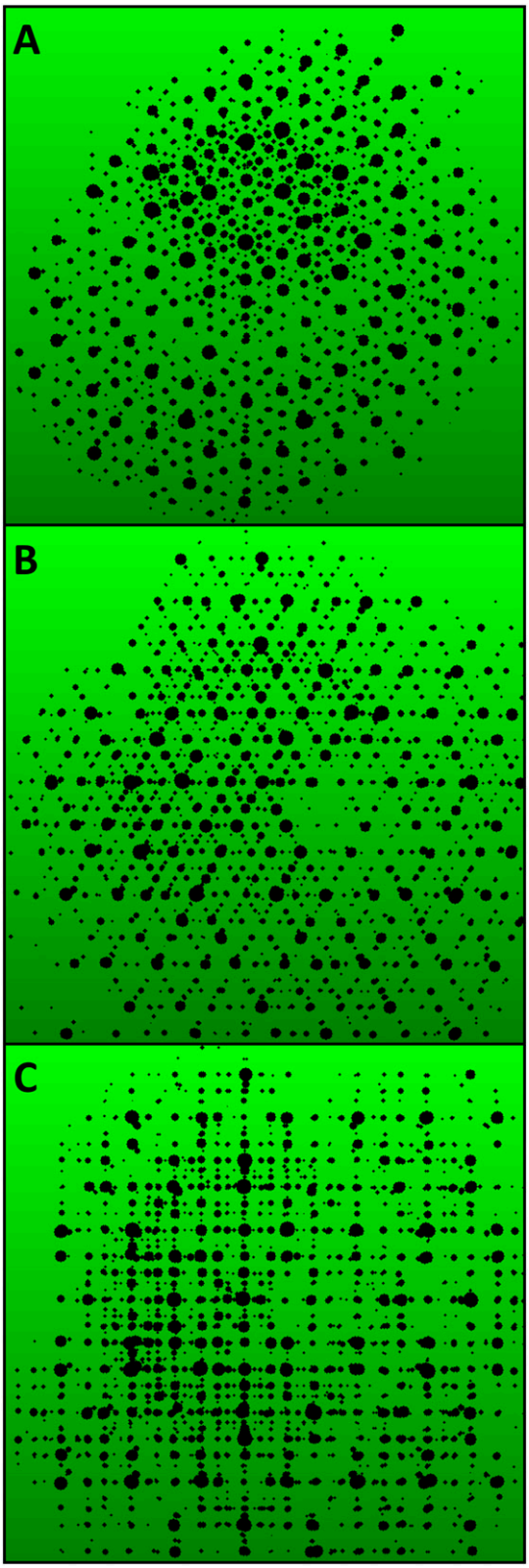

Fig. S2. Reconstructed precession figures from the single-crystal X-ray study of the i-phase grain. (*A*) Viewed down the fivefold symmetry axis. (*B*) Viewed down the threefold symmetry axis. (*C*) Viewed down the twofold symmetry axis. These patterns match those predicted for a face-centered icosahedral quasicrystal.

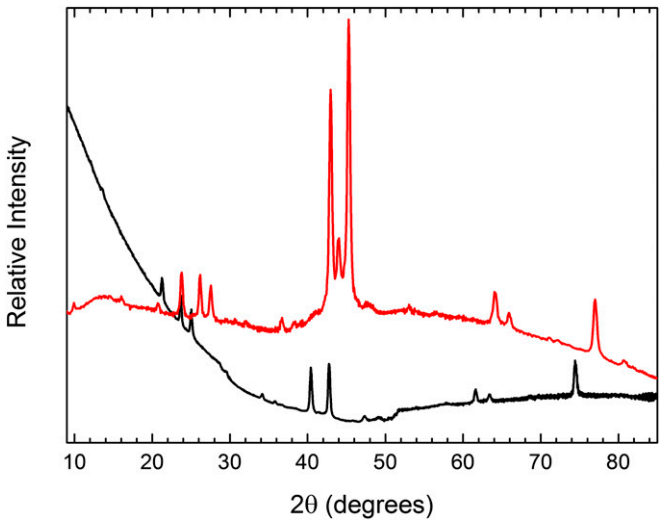

Fig. S3. Comparison of the powder XRD patterns of natural icosahedrite (red) (data courtesy of ref. 5) and the newly synthesized i-phase (black) (the present study). Although background subtraction for the small i-phase sample is imperfect, the similarity of patterns and the systematic peak shift to smaller 2θ angle in the new i-phase are evident.